Synthesis and Anti-inflammatory Properties of 1α,25-Dihydroxy-16-ene-20-cyclopropyl-24-*oxo*-vitamin D_3, a Hypocalcemic, Stable Metabolite of 1α,25-Dihydroxy-16-ene-20-cyclopropyl-vitamin D_3

Gilles Laverny,[†] Giuseppe Penna,[†] Milan Uskokovic,[‡] Stanislaw Marczak,[‡] Hubert Maehr,[‡] Pawel Jankowski,[‡] Caroline Ceailles,[§] Paul Vouros,[§] Brenden Smith,[||] Matthew Robinson,[||] G. Satyanarayana Reddy,[||,⊥] and Luciano Adorini*[,†]

BioXell, 20132 Milan, Italy, BioXell Inc., Nutley, New Jersey 07110, The Barnett Institute, Department of Chemistry, Northeastern University, Boston Massachusetts 02115, Epimer LLC, Providence, Rhode Island 02906, Department of Chemistry, Brown University, Box H, Providence, Rhode Island 02912

Received October 28, 2008

1α,25$(OH)_2$-16-ene-20-cyclopropyl-vitamin D_3 (**13**) is several fold more potent than the natural hormone 1α,25-dihydroxyvitamin D_3 (**1**) as an anti-inflammatory agent. Here, we have further analyzed the anti-inflammatory properties of **13**, confirming it as the most potent analogue tested within this family. We then determined the structures of all the natural metabolites of **13**, including the 24-*oxo* metabolite **14**, and carried out its synthesis. A comparison of **13** with **14** showed a similar induction of the primary VDR target genes *CYP24A1* and *CAMP* and comparable anti-inflammatory properties as revealed by a similar inhibition of TNF-α, IL-12/23p40, IL-6, and IFN-γ production. Interestingly, **14** displays a 3-fold lower calcemic activity in vivo compared to **13**. Collectively, these findings indicate that the strong potency of **13** can be explained by the accumulation of its stable 24-*oxo* metabolite, which shows immunoregulatory and anti-inflammatory properties superimposable to those exerted by **13** itself.

Introduction

1α,25-dihydroxyvitamin D_3 (**1**), the biologically active form of vitamin D_3, is a secosteroid hormone with a central role in calcium and bone metabolism. **1** also regulates growth and differentiation of many cell types and possesses exquisite immunoregulatory and anti-inflammatory properties.[1] The biological effects of **1** are mediated by the vitamin D receptor (VDR), a member of the superfamily of nuclear receptors.[2] VDR functions as a ligand-activated transcription factor that binds to specific vitamin D response elements in the promoter region of its primary target genes, modulating their rate of expression.[3] VDR agonists, which show benefit in several models of autoimmune and chronic inflammatory diseases, are the most used class of topical agents for the treatment of psoriasis, an autoimmune disease of the skin,[4] and are also recognized to have potential therapeutic value in other clinical conditions.[5−7] Because supraphysiologic concentrations of **1** and its analogues are usually required to exert immunosuppressive and antiproliferative effects, more than 3000 vitamin D_3 analogues with several different structural modifications have been synthesized during the past two decades.[8−10] Some of these analogues, such as elocalcitol (BXL-628), were found to have enhanced biological activity with less calcemic liability compared to **1**.[11] Elocalcitol was recently proposed for the treatment of benign prostatic hyperplasia[12] and clinically tested with good efficacy and excellent safety.[13]

Two classes of analogues with 16-ene or 20-cyclopropyl modification have become prominent because of their unique biological properties. Both classes of VDR[a] agonists have been shown to decrease cell proliferation and promote cell differentiation with a potency several orders of magnitude greater than that of **1**.[14,16] The potency of 20-cyclopropyl-vitamin D_3 analogues can be increased both in terms of their calcemic and immunomodulatory activities by the addition of a 16-ene moiety.[14] In the present study, we have further characterized the potency of this 16-ene-20-cyclopropyl family with respect to their anti-inflammatory properties by studying the inhibition of interferon-γ (IFN-γ) and tumor necrosis factor-α (TNF-α) in two different in vitro models. On the basis of these experiments, we have identified 1α,25$(OH)_2$-16-ene-20-cyclopropyl-vitamin D_3 (**13**) as the most potent anti-inflammatory compound among all the members of the 16-ene-20-cyclopropyl family tested.

Over a decade ago, we proposed that one of the mechanisms responsible for the enhanced biological activities of 1α,25$(OH)_2$-16-ene-vitamin D_3, when compared to **1**, is the difference in their target tissue metabolism.[15,16] On the basis of our earlier observations related to the target tissue metabolism of 1α,25$(OH)_2$-16-ene-vitamin D_3, we anticipated similarities between this compound and **13** in their target tissue metabolism. Therefore, we investigated the metabolism of **13** in rat osteosarcoma cells (UMR-106) and found **13** to be metabolized in the same way as 1α,25$(OH)_2$-16-ene-vitamin D_3.[14] We noted that **13** is metabolized in UMR-106 cells into a metabolite tentatively identified as the 24-*oxo* derivative.[14] Here, we unequivocally identify the stable metabolite of **13** as 1α,25$(OH)_2$-16-ene-20-cyclopropyl-24-*oxo*-vitamin D_3 (**14**). Chemical synthesis of **14** allowed a comparison of VDR-mediated activities and anti-

* To whom correspondence should be addressed. Phone: +39-075-7921934. Fax: +39-075-7921934. Mobile: +39-348-0172983. E-mail: LAdorini@interceptpharma.com. Address: Intercept Pharma, Via P. Togliatti 22 bis, 06073 Corciano (Perugia), Italy.

† BioXell.

‡ BioXell Inc.

§ The Barnett Institute, Department of Chemistry, Northeastern University.

|| Epimer LLC.

⊥ Department of Chemistry, Brown University.

[a] Abbreviations: IFN-γ, interferon-γ; TNF-α, tumor necrosis factor-α; CYP24A1, 25-hydroxyvitamin D-24-hydroxylase; CAMP, cathelicidin antimicrobial peptide; UMR-106, rat osteosarcoma cells; IL, interleukin; VDR, vitamin D receptor; CAOV, carcinoma ovarian; PBMC, peripheral blood mononuclear cells; THP-1, human acute monocytic leukemia cell line; LPS, lipopolysaccharide; MLR, mixed lymphocyte reaction; MTD, maximal tolerated dose; TLR4, Toll like receptor 4; Th, helper T cells.

10.1021/jm801365a CCC: $40.75
Published on Web 03/23/2009

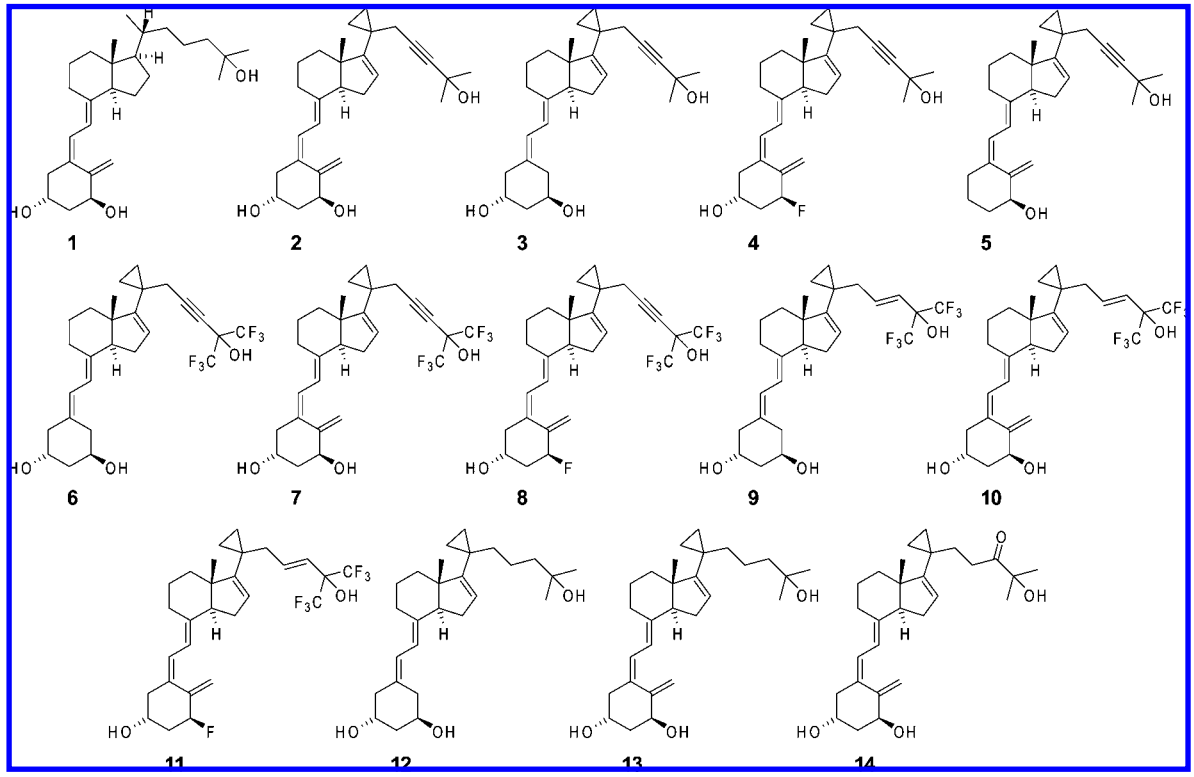

Figure 1. Chemical structures of 1α,25(OH)$_2$-vitamin D_3 (**1**) and various 16-ene-20-cyclopropyl-vitamin D_3 analogues used in this study.

Table 1. Inhibition of Pro-inflammatory Cytokines by 16-ene-20-cyclopropyl-vitamin D_3 Analogues[a]

chemical name	compd	MLR IFN-γ IC_{50}(pM)	LPS TNF-α IC_{50}(nM)
1,25-dihydroxy-vitamin D_3	**1**	29	8
1,25-dihydroxy-16-ene-23-yne-20-cyclopropyl-vitamin D_3	**2**	34	0.001
1,25-dihydroxy-16-ene-23-yne-20-cyclopropyl-19-nor-vitamin D_3	**3**	25	0.001
1α-fluoro-25-hydroxy-16-ene-23-yne-20-cyclopropyl-vitamin D_3	**4**	16	>100
3-desoxy-1,25-dihydroxy-16-ene-23-yne-20-cyclopropyl-vitamin D_3	**5**	562	ND
1,25-dihydroxy-16-ene-20-cyclopropyl-23-yne-26,27-hexafluoro-19-nor-vitamin D_3	**6**	14	>100
1,25-dihydroxy-16-ene-20-cyclopropyl-23-yne-26,27-hexafluoro-vitamin D_3	**7**	45	1
1α-fluoro-25-hydroxy-16-ene-20-cyclopropyl-23-yne-26,27-hexafluoro-vitamin D_3	**8**	585	ND
1,25-dihydroxy-16,23*E*-diene-20-cyclopropyl-26,27-hexafluoro-19-nor-vitamin D_3	**9**	12	>100
1,25-dihydroxy-16,23*E*-diene-20-cyclopropyl-26,27-hexafluoro-vitamin D_3	**10**	40	>100
1α-fluoro-25-hydroxy-16,23*E*-diene-20-cyclopropyl-26,27-hexafluoro-vitamin D_3	**11**	65	>100
1,25-dihydroxy-16-ene-20-cyclopropyl-19-nor-vitamin D_3	**12**	31	6
1,25-dihydroxy-16-ene-20-cyclopropyl-vitamin D_3	**13**	<0.00001	0.0002

[a] IFN-γ and TNF-α secretion were used as read-out for the MLR assay and LPS-stimulated PBMC assay, respectively. The results demonstrate that **13** is the most potent inhibitor of IFN-γ and TNF-α secretion among the 16-ene-20-cyclopropyl-vitamin D_3 analogues tested. Assays were performed as described in the Experimental Section. ND, not determined.

inflammatory properties of **14** with its parent compound **13**. The available data indicate that the accumulation of the active 24-*oxo* metabolite **14** in target tissues could explain the high potency of **13**. Further, we also found that the potency of **14** to increase serum calcium levels is three times lower than that of **13**, indicating that **14** represents an anti-inflammatory agent with a wider therapeutic window than its parent **13**.

Results

Potent Anti-inflammatory Properties of 1α,25(OH)$_2$-16-ene-20-cyclopropyl-vitamin D_3 (13) Compared to Other 16-ene-20-cyclopropyl Vitamin D_3 Analogues. In our recent study, we assessed the anti-inflammatory property of several 16-ene-20-cyclopropyl-vitamin D_3 analogues in an assay measuring the inhibition of IFN-γ production and found that **13** is several fold more potent than **1**.[14] In the present study, we reassessed **13**, along with several other 16-ene-20-cyclopropyl-vitamin D_3 analogues (Figure 1), for their anti-inflammatory properties by assessing their ability to inhibit two key pro-inflammatory cytokines, namely TNF-α and IFN-γ; the results are summarized in Table 1. Most of the 16-ene-20-cyclopropyl-vitamin D_3 analogues inhibited IFN-γ with an IC_{50} similar to that of **1** (IC_{50} = 29 pM), but **13** showed a much stronger potency in the inhibition of IFN-γ production ($IC_{50} < 10^{-5}$ pM). While 16-ene-20-cyclopropyl-vitamin D_3 analogues inhibited IFN-γ similarly to **1**, the inhibition of TNF-α showed wide differences. Some compounds failed to induce TNF-α inhibition like 1α-fluoro-25-hydroxy-16-ene-23-yne-20-cyclopropyl-vitamin D_3 (**4**), 1α,25(OH)$_2$-16-ene-20-cyclopropyl-23-yne-26,27-hexafluoro-19-nor-vitamin D_3 (**6**), 1α,25(OH)$_2$-16,23*E*-diene-20-cyclopropyl-26,27-hexafluoro-19-nor-vitamin D_3 (**9**), 1α,25(OH)$_2$-16,23*E*-diene-20-cyclopropyl-26,27-hexafluoro-vitamin D_3 (**10**), and 1α-fluoro-25-hydroxy-16,23*E*-diene-20-cyclopropyl-26,27-hexafluoro-vitamin D_3 (**11**) ($IC_{50} > 10^{-7}$ M), whereas others inhibited TNF-α more efficiently than **1**, irrespective of a similar inhibitory capacity of IFN-γ production. Conversely, **13** inhib-

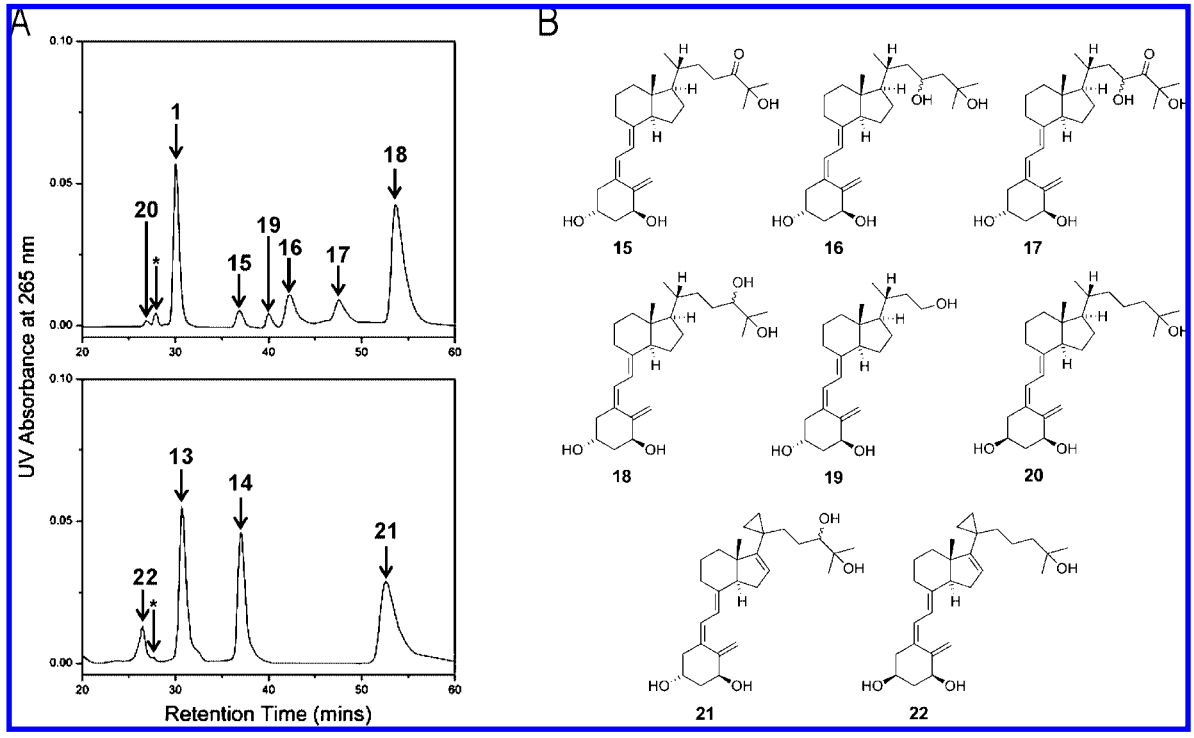

Figure 2. Identification of the various metabolites of 1α,25-dihydroxyvitamin D_3 (**1**) and 1α,25$(OH)_2$-16-ene-20-cyclopropyl-vitamin D_3 (**13**). (A) HPLC profiles of the lipid extracts of various vitamin D metabolites produced in CAOV cells incubated with **1** (upper panel) and **13** (lower panel). HPLC was performed using a Zorbax-SIL column (9−250 nm) eluted with hexane−isopropanol (90:10) at a flow rate of 2 mL/min. The various metabolites of **1** and **13** were monitored by their UV absorbance at 265 nm, and each metabolite is represented by a number. The peak represented by the asterisk is pre-**1** in the upper panel and pre-**13** in the lower panel. (B) Chemical structures of various metabolites of **1** and **13** are as follows: 1α,25$(OH)_2$-24-*oxo*-vitamin D_3 (**15**), 1α,23,25$(OH)_3$-vitamin D_3 (**16**), 1α,23,25$(OH)_3$-24-*oxo*-vitamin D_3 (**17**), 1α,24,25$(OH)_3$-vitamin D_3 (**18**),1α,23$(OH)_2$-24,25,26,27-tetranor-vitamin D_3 (**19**), 1α,25$(OH)_2$-3-epi-vitamin D_3 (**20**), 1α,24,25$(OH)_3$-16-ene-20-cyclopropyl-vitamin D_3 (**21**), 1α,25$(OH)_2$-24-*oxo*-16-ene-20-cyclopropyl-vitamin D_3 (**14**), 1α,25$(OH)_2$-16-ene-20-cyclopropyl-3-epi-vitamin D_3 (**22**).

ited IFN-γ and TNF-α production with an $IC_{50} < 10^{-17}$ M and 2×10^{-13} M, respectively.

Thus, the present data provide convincing evidence to indicate **13** as the most potent anti-inflammatory agent of all the 16-ene-20-cyclopropyl-vitamin D_3 analogues tested.

Production of Various Metabolites of 13 in CAOV Cells. In our previous study, we compared the metabolism of two 20-cyclopropyl analogues, namely 1α,25$(OH)_2$-20-cyclopropyl-vitamin D_3 and **13** in UMR 106 cells.[14] The metabolism data generated in UMR 106 cells indicated that 1α,25$(OH)_2$-20-cyclopropyl-vitamin D_3 was rapidly metabolized through three different pathways (24-oxidation, C-3 epimerization, and C-1 esterification pathways) and the pattern of metabolism was similar to that of 1α,25$(OH)_2$-20-epi-vitamin D_3 previously studied in our laboratory (**17**). Conversely, **13** was mainly metabolized through only two pathways (C-24 oxidation and C-3 epimerization pathways). On the basis of the preliminary data, we concluded that **13** attains higher biological potency over 1α,25$(OH)_2$-20-cyclopropyl-vitamin D_3 because of its metabolic stability. However, in our previous study, we could not unequivocally identify all the metabolites of **13**, including its 24-*oxo* metabolite **14**. Therefore, we undertook the present study to produce the various natural metabolites of **13** in human ovarian cancer cells (CAOV cells), which were previously shown to express high 24-hydroxylase activity (S. Reddy et al., unpublished observations).

The HPLC profiles of all of the metabolites of **1** (upper panel) and **13** (lower panel) produced by CAOV cells during a 24 h incubation period are shown in Figure 2A. The chemical structures of all the metabolites of **1** and **13** are shown in Figure 2B. **1** was metabolized into several polar metabolites via the C-23 and C-24 oxidation pathways as well as through the C-3 epimerization pathway. The pattern of metabolism of **1** into its various metabolites is similar to those reported previously.[33] However, the pattern of the metabolism of **13** is different. Upon careful examination, it becomes obvious that most of the starting substrate of **13** is converted into 24-hydroxy- (**21**) and 24-*oxo*- (**14**) metabolites, which accumulate significantly. Along with metabolites **21** and **14**, we also noted the production of a less polar metabolite **22**, which is identified as 1α,25$(OH)_2$-16-ene-20-cyclopropyl-3-epi-vitamin D_3.

In conclusion, it appears that a significant proportion of the biological activity of **13** may be due to its conversion into stable intermediary metabolites.

Structure Identification of All the Natural Metabolites of 13. Finally, we succeeded in producing all three metabolites of **13** in quantities sufficient for their structure identification. Data in Figure 3 show the mass spectra obtained for the trimethylsilylated **13** substrate and its three metabolites.

The mass spectrum of trimethylsilylated **13** substrate shown in Figure 3A exhibited a molecular ion at *m*/*z* 642. The fragments at *m*/*z* 552 and 462 were formed by sequential elimination of one and two trimethylsilanol moieties from *m*/*z* 642. Ion fragments at *m*/*z* 511 (loss of 131 Da from the molecular ion) and *m*/*z* 217 arised from cleavage of the A ring, as depicted in Figure 3A. Cleavage of the side chain (C24−C25) yielded a characteristic ion fragment at *m*/*z* 131.

The trimethylsilylated metabolite **22** (Figure 3B) exhibited virtually identical mass spectral characteristics as the trimethylsilylated substrate (Figure 3A), but the GC retention time (15.16 min) did not match that of the trimethylsilylated substrate (14.51 min). These observations indicated that both compounds

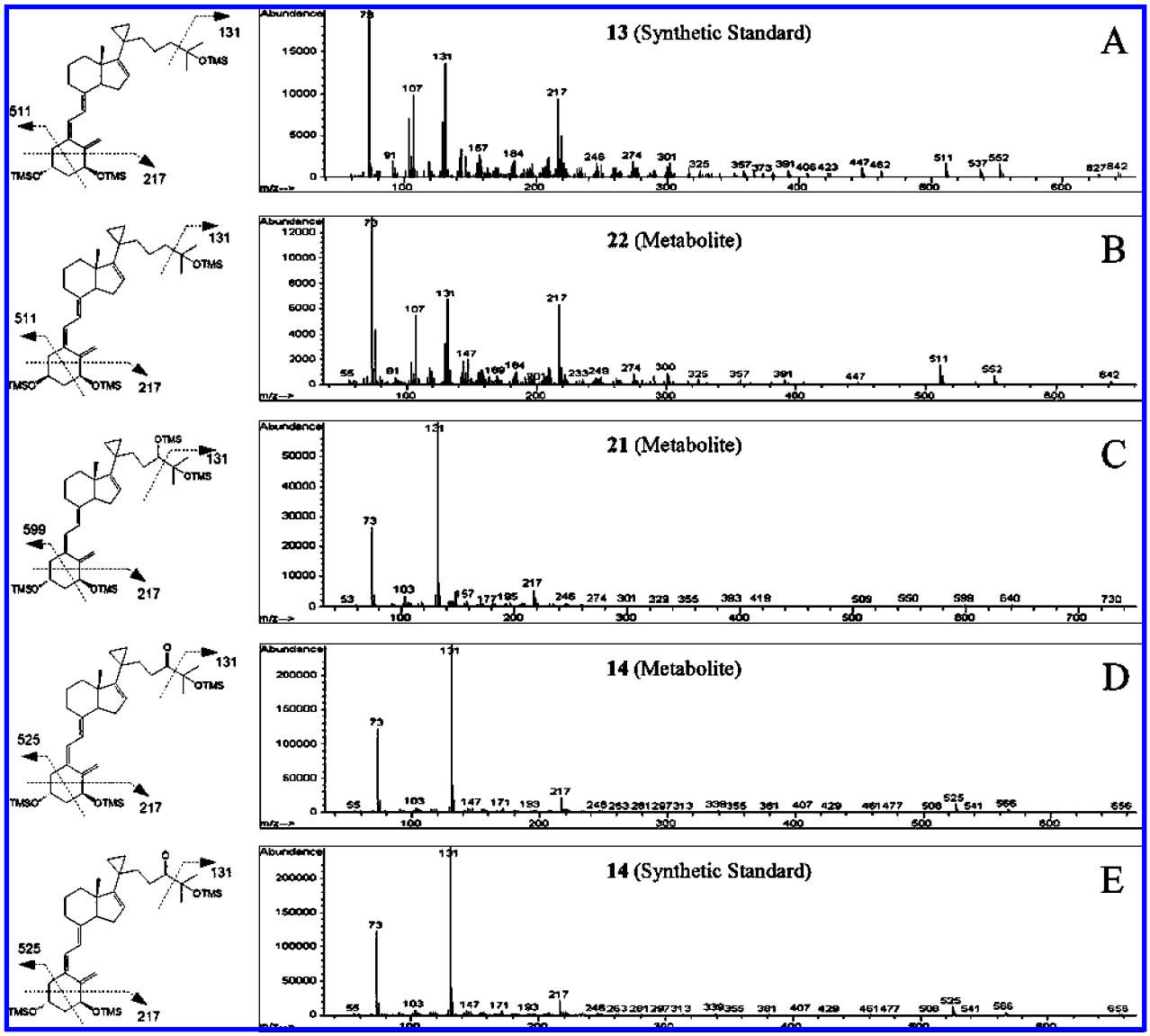

Figure 3. Structure identification of all the natural metabolites of **13**. GC-MS analysis was performed using an Agilent GC System 6890 equipped with a mass selective detector MSD5973. All analyses were performed as described in the Experimental Section.

must be stereoisomers, in agreement with the proposed identification of metabolite **22** as the 3-epimer of the substrate, namely 1α,25$(OH)_2$-16-ene-20-cyclopropyl-3-epi-vitamin D_3 (**22**), product of the C-3 epimerization pathway.

The mass spectrum of trimethylsilylated metabolite **21** shown in Figure 3C revealed a molecular ion at *m*/*z* 730, which, when compared to the substrate, indicated the incorporation of a hydroxyl group (-OTMS after derivatization). The peak at *m*/*z* 599 (M-131) and the presence of a fragment at *m*/*z* 217 confirmed that the A ring remained unmodified. These observations were in agreement with the assigned structure, **21**.

Identical mass spectral characteristics were observed for the trimethylsilylated **14** synthetic standard (Figure 3E) and for the trimethylsilylated metabolite **14** (Figure 3D). Both trimethylsilylated derivatives exhibited molecular ions at *m*/*z* 656 as well as the characteristic ion fragments at *m*/*z* 525 (M-131) and *m*/*z* 217 (A ring cleavage) and *m*/*z* 131 (side chain cleavage). In addition to the identical mass spectra, the GC retention time (rt) on GC-MS confirmed the identity of **14** (rt = 15.19 min), which was identical to that of the synthetic standard.

Synthesis of 14. The synthesis of **13** was recently disclosed by our group.[14] The preparation of its 24-*oxo* metabolite **14** was secured by a series of standard reactions, as shown in Scheme 1. Condensation of the CD-ring moiety **23** with acetone in the presence of butyl lithium as base produced the tertiary alcohol **24**. The desired 24-*oxo* group in **25** was then formed by alkyne hydration with sulfuric acid and mercury oxide. Oxidation of the secondary alcohol and protection of the tertiary alcohol generated **26** needed for the coupling with ring A precursor **27** to produce **14** after deprotection.

Similar Induction of Primary VDR Target Genes by 13 and its 24-*oxo* Metabolite 14. To address the possibility that the metabolism of **13** into a stable bioactive metabolite could explain its higher potency, we first compared the ability of **13** and its 24-*oxo* metabolite **14** to induce primary VDR target genes in two different human cell culture systems, peripheral blood mononuclear cells (PBMCs) and human acute monocytic leukemia cells (THP-1 cells). As shown in Figure 4A, a dose−response titration at low concentrations of VDR agonists in PBMCs showed at 10 pM and 100 pM, but not at 1 pM, a significantly higher increase of transcripts encoding 25-hydroxyvitamin D-24-hydroxylase (*CYP24A1*) and cathelicidin antimicrobial peptide (*CAMP*) by both **13** and **14** compared to **1**. Then, to study if the higher potency of these two compounds

Scheme 1. Summary of the Synthesis of **14**

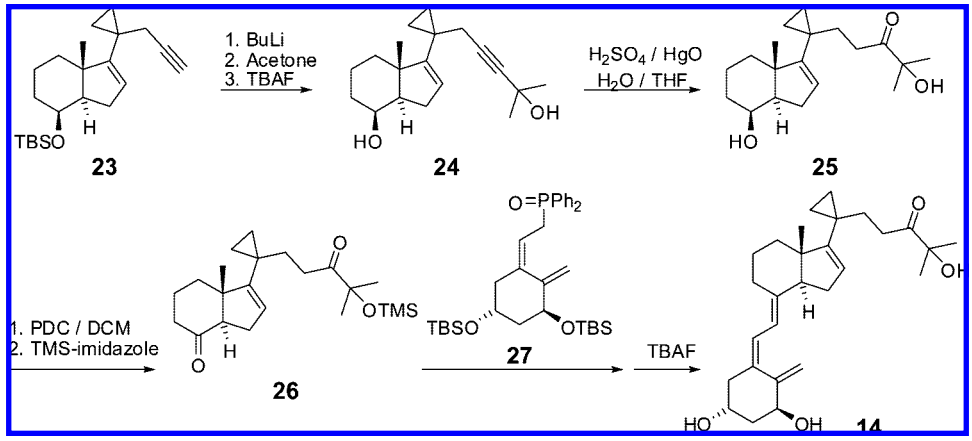

results in a modification of the kinetics of VDR signaling, we measured the induction of *CYP24A1* mRNA at a saturating dose (10 nM) of **13**, **14**, and **1** over a time course of 8 h. As shown in Figure 4B, all the three VDR agonists induced *CYP24A1* mRNA similarly at all time points analyzed, indicating that the higher potency of both **13** and **14** when compared to **1** is mainly due to the capacity of **13** and **14** to activate the VDR at lower concentrations.

Potential differences in VDR signaling could be masked by the variability between donors and by the saturation of the system. For these reasons, we performed a time-course analysis of the induction of primary VDR target genes in THP-1 cells using a common nonsaturating concentration of each VDR agonist and determined EC_{50} value for each compound. Results obtained using this model system (Figure 5A) confirmed that **13** and **14** possess a similar capacity to induce the primary VDR target genes *CYP24A1* and *CAMP* (EC_{50} values of 6.8×10^{-10} M and 6.9×10^{-10} M, respectively), with a potency significantly higher than that of **1** ($EC_{50} = 1 \times 10^{-8}$ M). As previously shown in PBMCs (Figure 4B), induction of *CYP24A1* and *CAMP* mRNA in THP-1 cells proceeded with the same kinetics for the three VDR agonists tested at their EC_{50} concentrations, confirming that **13** and **14** are indeed more potent than **1** (Figure 5B).

Similar Immunomodulatory Properties of 13 and its 24-*oxo* Metabolite 14. To compare the immunomodulatory properties of **13** with **14**, we evaluated the potency of the three VDR agonists **13**, **14**, and **1** to inhibit the production of two key pro-inflammatory cytokines, IFN-γ and TNF-α. The inhibitory activities of **13** and **14** on IFN-γ production in the MLR assay are perfectly superimposable, and both compounds are significantly more potent than **1** ($IC_{50} < 10^{-12}$ M and 2.5×10^{-11} M, respectively) (Figure 6A). Production of TNF-α was also similarly inhibited by **13** and **14** in LPS-stimulated PBMCs, and both compounds were again significantly more potent than **1** (Figure 6B). We then studied the expression of *TNF*-α mRNA using the same conditions previously used to study the expression of *CYP24A1* mRNA (Figure 4B). We noted that the expression of *TNF*-α mRNA in LPS-activated PBMCs was inhibited to the same extent and with similar kinetics by all the three VDR agonists (**13**, **14**, and **1**) at 10 nM concentration (Figure 6C).

To further compare the anti-inflammatory properties of **13** and **14**, we also carried out extended dose−response curves analyzing the production of two other key pro-inflammatory cytokines, IL-12/23p40 (Figure 7A) and IL-6 (Figure 7B). **13** and **14** are again indistinguishable in their inhibitory activity in LPS-activated PBMCs and showed a significantly lower IC_{50}

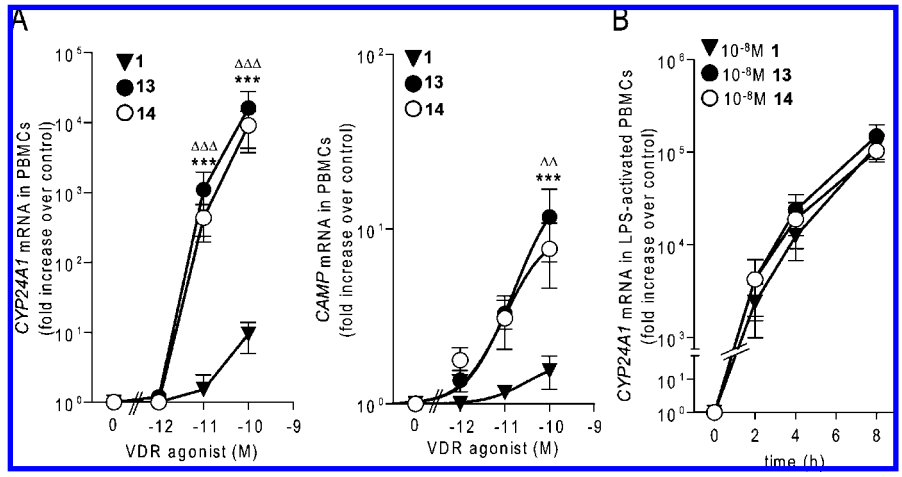

Figure 4. Induction of primary VDR response genes by **1**, **13**, and its 24-*oxo* metabolite **14**. (A) Induction of *CYP24A1* and *CAMP* transcripts after overnight incubation of PBMCs with the indicated concentrations of VDR agonists. (B) Time course of *CYP24A1* mRNA induction in 24 h LPS-stimulated PBMCs by 10 nM of the indicated VDR agonists. Data have been obtained as described in Experimental Section. Values are expressed in arbitrary units where 1 represents gene expression in the absence of VDR agonists. **13** vs **1**, $***P < 0.001$; **14** vs **1**, $\Delta\Delta P < 0.01$, $\Delta\Delta\Delta P < 0.001$.

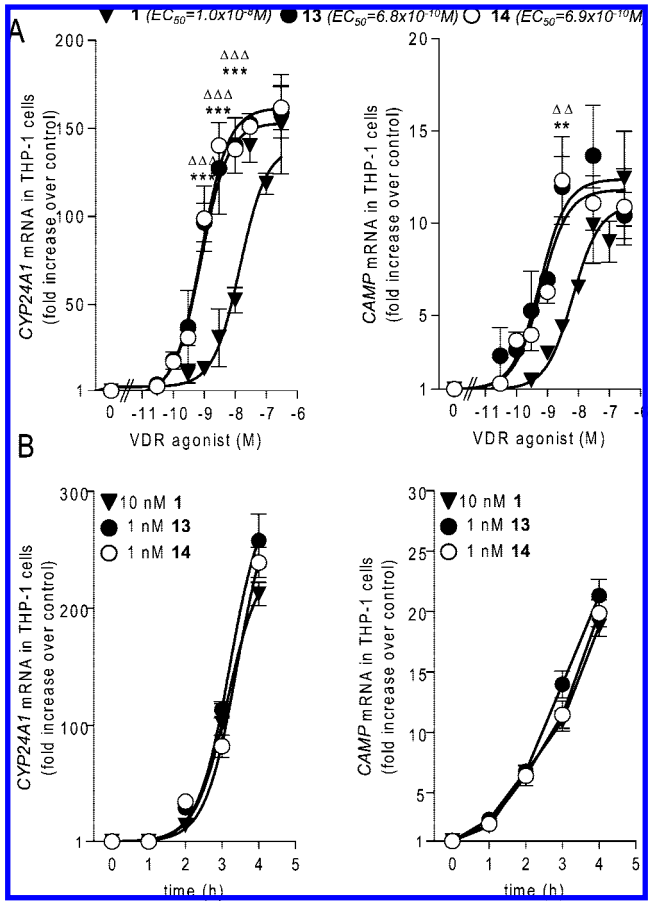

Figure 5. Equal potency of **13** and its 24-*oxo* metabolite **14** in the induction of primary VDR response genes in THP-1 cells. (A) Expression of *CYP24A1* and *CAMP* mRNA in THP-1 cells after a 4 h incubation with the indicated concentrations of VDR agonists. (B) Time course of *CYP24A1* and *CAMP* mRNA induction by 10 nM **1**, 1 nM **13**, or 1 nM **14**. Data have been obtained as described in the Experimental Section. Values are expressed in arbitrary units, where 1 represents gene expression in the absence of VDR agonists. **13** vs **1**, $^{**}P < 0.01$, $^{***}P < 0.001$; **14** vs **1**, $\Delta\Delta P < 0.01$, $\Delta\Delta\Delta P < 0.001$.

value compared to **1** for production of IL-12/23p40 (**13**: $<10^{-12}$ M; **14**: $< 10^{-12}$ M; **1**: 10^{-9} M) and IL-6 (**13**: 3.2×10^{-9} M; **14**: 3.5×10^{-9} M; **1**: 1.2×10^{-8} M). These data, together with the similar up-regulation of primary VDR response genes, indicate that **13** and **14** possess a similar activity in all the assays performed. These findings suggest that the VDR-dependent effects induced by **13** may actually be mediated by its 24-*oxo* metabolite.

Lower Calcemic Activity of 14 Compared to 13 and 1. The in vivo calcemic activities of **14**, **13**, and **1** were assessed by measuring the capacity of each compound at different doses to induce hypercalcemia in the mouse after a single oral administration of each dose for four consecutive days. Results in Figure 8 show that the maximum tolerated dose (MTD) for **1** is 0.3 μg/kg, and for **13** is 1 μg/kg, whereas the MTD for **14** is 3 μg/kg. These results indicate that **14** is the least hypercalcemic among the three VDR agonists tested.

Discussion

Structural and stereochemical modifications at C-20 significantly influence the biological effects of **1** and its analogues.[14] 1α,25(OH)$_2$-20-epi-vitamin D_3 exhibits up to 5000 times greater antiproliferative activity than **1** in various cancer cell lines without increased hypercalcemic properties.[17] Crystal structure analysis of the VDR-1α,25(OH)$_2$-20-epi-vitamin D_3 complex indicated that additional contacts of the ligand within the ligand-binding pocket of the VDR contributed to enhanced stability and longer half-life.[18] This led us to the synthesis of 20-cyclopropyl analogues, which mimic the methyl groups of **1** and its 20-epi analogue. During the course of these studies, we noted that introduction of the 16-ene modification into our VDR agonist library of 20-cyclopropyl vitamin D_3 analogues increases their potency both in terms of calcemic and immunomodulatory activities.[14]

In the present study, we reassessed the immunomodulatory actions of several 16-ene-20-cyclopropyl-vitamin D_3 analogues using two different in vitro assays, the MLR and the activation of PBMCs induced by LPS, and identified **13** as the analogue with the highest potency to inhibit the production of two key pro-inflammatory cytokines, IFN-γ and TNF-α.

The MLR assay is used as an in vitro model of adaptive immunity and is widely applied to monitor diseases, such as AIDS,[19] to predict transplant rejection, especially in renal transplantation,[20] and to screen for novel immunosuppressive drugs.[21] An important cytokine produced in a MLR assay is IFN-γ, a cytokine directly regulated by VDR agonists.[22] IFN-γ is the signature cytokine of Th1 cells, a cell subset pathogenic in different conditions, including autoimmune diseases.[23] Th1 cells are strongly inhibited by VDR agonists, both directly and indirectly via inhibition of IL-12 production by antigen-presenting cells.[24,25] The very potent inhibitory activity exerted on IFN-γ production by 16-ene-20-cyclopropyl compounds, and in particular by **13**, demonstrates their marked immunoregulatory properties.

One of the mechanisms regulating innate immunity involves the TLRs, pattern recognition receptors playing a crucial role in early host defense against invading pathogens.[26] In our experiments, we focused on toll-like receptor 4 (TLR4) because its ligand, the bacterial endotoxin LPS, is a potent inducer of immune responses.[27] We have analyzed the pro-inflammatory cytokine TNF-α, which is produced after the activation of TLR4. TNF-α plays a key role in many disorders, such as rheumatoid arthritis, acute lung injury, and inflammatory bowel disease,[28] and anti-TNF-α biologicals are clinically used for the treatment of several autoimmune diseases.[29] Our data show that **13** is a potent inhibitor of TNF-α. These findings indicate that **13** is an extremely potent and versatile immunomodulatory compound targeting key pathogenic effector cells. Moreover, its MTD, which is three times higher than **1**, would provide a wider therapeutic window for **13** over **1**.

It is now well established that **1** is metabolized by CYP24A1, a multicatalytic enzyme, in various target tissues.[33,34] Over a decade ago, we identified differences in the metabolism between 1α,25(OH)$_2$-16-ene-vitamin D_3 and **1** and recognized that minor alterations in the structure of **1** can produce major changes in its target tissue metabolism. We noted that the introduction of 16-ene modification into **1** possibly produces a conformational change in the side chain, which allows efficient C-24 hydroxylation and C-24 oxidation but not C-23-hydroxylation.[15,16] As a result, the 24-*oxo* metabolite of 1α,25(OH)$_2$-16-ene-vitamin D_3 accumulates in increasing amounts in target tissues when compared to the corresponding 24-*oxo* metabolite of **1**. We then investigated the biological activity of the stable 24-*oxo* metabolite of 1α,25(OH)$_2$-16-ene-vitamin D_3 to clarify if some of the actions of 1α,25(OH)$_2$-16-ene-vitamin D_3 may indeed be accounted for by its stable 24-*oxo* metabolite. Indeed, 1α,25(OH)$_2$-16-ene-vitamin D_3 and its 24-*oxo* metabolite were found to be

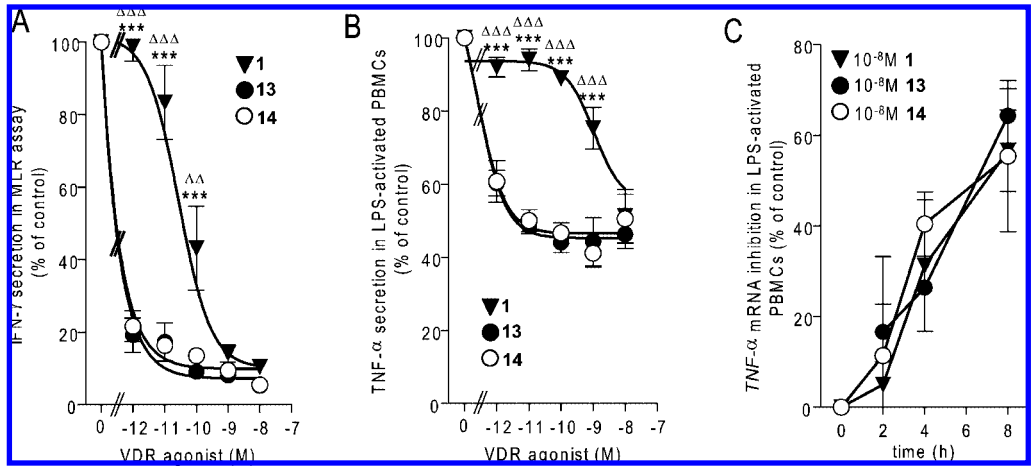

Figure 6. Equal potency of **13** and its 24-*oxo* metabolite **14** in the inhibition of IFN-γ and TNF-α production. (A) Allogeneic PBMCs were cultured in a bidirectional MLR assay for 5 days with the indicated concentrations of VDR agonists. At the end of the culture period, IFN-γ production was measured in culture supernatants by two-site ELISA. Assays were performed as described in the Experimental Section. Results are expressed as percent of cytokine production in the absence of VDR agonists. (B) Inhibition of TNF-α secretion in LPS stimulated PBMCs. (C) Inhibition of *TNF*-α mRNA by 10 nM of the indicated VDR agonists. Each point represents the mean ± SEM of at least three independent experiments. **13** vs **1**, ***$P < 0.001$; **14** vs **1**, ΔΔ$P < 0.01$, ΔΔΔ$P < 0.001$.

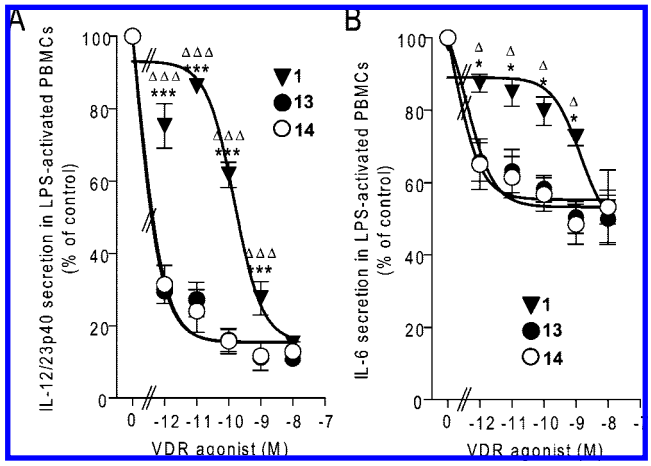

Figure 7. Equal potency of **13** and its 24-*oxo* metabolite **14** in the inhibition of IL-12/23p40 and IL-6 in LPS stimulated PBMCs. (A) Inhibition of IL-12/23p40 secretion. (B) Inhibition of IL-6 secretion. Data have been obtained as described in the Experimental Section. Results are expressed as percent of cytokine production in the absence of VDR agonists. Each point represents the mean ± SEM of at least three independent experiments. **13** vs **1** *$P < 0.05$, **$P < 0.01$, ***$P < 0.001$; **14** vs **1**, Δ$P < 0.05$, ΔΔ$P < 0.01$, ΔΔΔ$P < 0.001$.

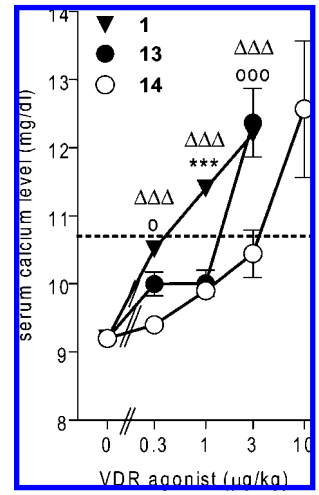

Figure 8. Calcemic activity of **14** compared to **13**. Eight week-old female C57BL/6 mice (3 mice/group) were dosed orally (0.1 mL/mouse) with various concentrations of VDR agonists daily for four days. Serum calcium levels were determined on day five using a colorimetric assay. Dotted plot represent the maximum normo-calcemic concentration (= 10.7 mg/mL) **13** vs **1**, ***$P < 0.001$; **14** vs **1**, ΔΔΔ$P < 0.001$; **14** vs **13**, O$P < 0.05$, OOO$P < 0.001$.

equipotent in inducing growth inhibition and promoting differentiation of RWLeu-4 human myeloid leukemic cells.[16] These data thus support the concept that one of the important mechanisms responsible for the increase in the potency of some of the vitamin D analogues can be due to their metabolism through alternative pathways leading to the production of stable and bioactive metabolites. On the basis of these earlier observations, we recently compared the metabolism of 1α,25(OH)$_2$-20-cyclopropyl-vitamin D$_3$ with that of **13** and showed that 1α,25(OH)$_2$-20-cyclopropyl-vitamin D$_3$ is rapidly metabolized through three different pathways (24-oxidation, C-3 epimerization and C-1 esterification pathways),[14] with a pattern of metabolism similar to that of 1α,25(OH)$_2$-20-epi-vitamin D$_3$.[17] Conversely, **13** is mainly metabolized through only two pathways (C-24 oxidation and C-3 epimerization pathways). On the basis of these preliminary data, we concluded that **13** can attain higher biological potency over 1α,25(OH)$_2$-20-cyclopropyl-vitamin D$_3$ because of its metabolic stability. In the present study, we investigated the metabolism of 1α,25(OH)$_2$-20-cyclopropyl-16-ene-vitamin D$_3$ in CAOV cells and confirmed that the 24-*oxo* metabolite **14** is indeed the final, stable metabolite. The chemical synthesis of **14** allowed us to assess its various biological properties.

To clarify if some of the actions of **13** may indeed be accounted for by its 24-*oxo* metabolite **14**, we first determined the potency of both **13** and **14** to modulate the induction of primary VDR target genes. Expression of *CYP24A*1, the most responsive primary VDR target gene, is similarly induced by **14** and **13** at the mRNA level both in terms of dose−response curves and timing of gene induction. Expression of *CAMP*, another primary VDR target gene is also modulated by **13** and **14** in the same way as *CYP24A1*.[35] As cathelicidin plays an important role in innate immunity,[36−38] these data indicate comparable properties for **13** and **14** in the regulation of innate immune responses. We then compared the anti-inflammatory properties of **13** and **14** by evaluating their ability to inhibit

IFN-γ and TNF-α along with two additional pro-inflammatory cytokines, IL-12/23p40 and IL-6. Both IL-12/23p40 and IL-6 also play an important role in immunomodulation. IL-12/23p40 is a component of the IL-12 heterodimer, which drives Th1 cell development,[30] but the IL-12p40 subunit can also bind to p19 and form IL-23, a cytokine sustaining the amplification of Th17 cells, a pathogenic T cell subset recognized to play a major role in the pathogenesis of autoimmune diseases.[31] IL-6 is a pleiotropic inflammatory cytokine that is also involved in the induction of Th17 cells, which in addition to IL-17 also produce IL-6 and TNF-α.[32] Interestingly, we noted that both **14** and **13** were equipotent in their ability to inhibit the production of TNF-α, IL-12/23p40, and IL-6, whereas **13** inhibited the production of IFN-γ more efficiently than **14** at their lowest concentrations. This difference could be due to the target cytokine or possibly to the assay used because, while effects on mRNA up-regulation and protein inhibition are similar in a 24 h assay, a slight difference was observed in the 5-d MLR model.

In summary, we have shown that the strong induction of primary VDR response genes and immuno-regulatory activities of **14** are comparable to those exerted by its parent compound **13**. Collectively, these findings indicate that the strong potency of **13** can be explained by the accumulation of its stable 24-*oxo* metabolite that displays immunoregulatory and anti-inflammatory properties superimposable to those exerted by **13** itself. However, we found that the MTD of **14** is three times higher than its parent compound **13**, indicating that the potency of the metabolite compared to the parent compound to induce hypercalcemia was reduced. On the basis of these findings, we now propose that **14** represents a better anti-inflammatory agent than its parent **13** due to its wider therapeutic window.

Conclusion

We have identified **13** as a VDR agonist with the highest potency to inhibit pro-inflammatory cytokine production among members of the 16-ene-20-cyclopropyl family. This compound is metabolized to **14**, which resists further metabolism. As a result, this 24-*oxo* metabolite of **13** accumulates in tissues. By combining our observations of equipotency between **13** and **14** in transcript regulation, and similar inhibition of cytokine production, we conclude that accumulation of **14** can explain the strong potency of **13**, supporting the concept that specific differences in the target tissue metabolism of VDR agonists can play a critical role to increase their potency.

Experimental Section

Chemistry. Synthesis and Characterization (NMR, NP-HPLC, MS, Elemental Analysis) of Target Compounds. NMR spectra were obtained with a Varian 400 MHZ spectrometer and the chemical shifts are reported in parts per million (ppm). The abbreviations used are as follows: s, singlet; bs, broad singlet; d, doublet; dd, double doublet; m, multiplet. Flash column chromatography was performed using Merck silica gel 60 (0.040−0.063 mm). TLCs were carried out on precoated TLC plates with silica gel 60 F-254 (Merck). All reactions were carried out under a nitrogen atmosphere. The purity of the tested compounds was determined by HPLC analysis and results were ≥95% purity unless otherwise stated. The analytical HPLC measurements were made according to: method (A) NP-HPLC, Zorbax-SIL, 9.4 mm × 25 cm, 9:1 hexane: isopropanol, flow rate 2 mL/min, UV 265 nM, charge 10 μg; method (B) RP-HPLC, Zorbax-ODS, 4.6 mm × 25 cm, 85:15 acetonitrile:methylene chloride, flow rate 2 mL/min, UV 265 nM, charge 10 μg.

(3a*R*,4*S*,7a*S*)-1-[1-(4-Hydroxy-4-methyl-pent-2-ynyl)-cyclopropyl]-7a-methyl-3a,4,5,6,7,7a-hexahydro-3*H*-inden-4-ol (24). To a stirred solution of **23** (1.0 g, 2.90 mmol) in tetrahydrofuran (15 mL) at −78 °C was added *n*-BuLi (2.72 mL, 4.35 mmol, 1.6 M in hexane).[37] After stirring at −78 °C for 1 h, acetone (2.5 mL, 34.6 mmol) was added and stirring was continued for 2.5 h. A saturated aqueous solution of ammonium chloride was added (15 mL), and the mixture was stirred for 15 min at room temperature and then extracted with ethyl acetate (2−50 mL). The combined extracts were washed with brine (50 mL) and dried (Na_2SO_4). The residue, obtained after evaporation of the solvent (2.4 g), was flash-chromatographed using 10% ethyl acetate in hexane as mobile phase to give the tertiary alcohol (1.05 g, 2.61 mmol), which was treated with tetrabutylammonium fluoride (6 mL, 6 mmol, 1.0 M in THF) and stirred at 65−75 °C for 48 h. The mixture was diluted with ethyl acetate (25 mL) and washed with water (5 × 25 mL) and brine (25 mL). The combined aqueous washes were extracted with ethyl acetate (25 mL), and the combined organic extracts were dried (Na_2SO_4). The residue, after evaporation (1.1 g), was flash-chromatographed (20% ethyl acetate in hexane) to give **24** (0.75 g, 2.59 mmol, 90%) $[\alpha]^{30}_D$ +2.7 (c 0.75, $CHCl_3$). ^{1}H NMR ($CDCl_3$): 5.50 (1H, m), 4.18 (1H, m), 2.40 (2H, s), 2.35−1.16 (11H, m), 1.48 (6H, s), 1.20 (3H, s), 0.76−0.50 (4H, m). ^{13}C NMR ($CDCl_3$): 156.39, 125.26, 86.39, 80.19, 69.21, 65.16, 55.14, 46.94, 35.79, 33.60, 31.67, 29.91, 27.22, 19.32, 19.19, 17.73, 10.94, 10.37. HRMS (EI) calcd for $C_{22}H_{28}O_2$ (M+) 288.2089, obsd 288.2091.

4-Hydroxy-1-[1-((3a*R*,4*S*,7a*S*)-4-hydroxy-7a-methyl-3a,4,5,6,7,7a-hexahydro-3*H*-inden-1yl)-cyclopropyl]-4-methyl-pentan-3-one (25). The mixture of **24** (250 mg, 0.87 mmol), THF (4 mL), and 6 drops of mercuric salts mixture (made by stirring at 65−70 °C of: 150 mg of HgO, 0.1 mL of concentrated sulfuric acid, 1.3 mL water, and 3.8 mL of methanol) was stirred at room temperature for 7 d with addition of 6 drops of mercuric salts mixture each day. Sodium hydrogen carbonate (0.5 g) was added and the reaction mixture filtered after 3 h; the solids were washed with Et_2O (50 mL). The filtrates were evaporated and the residue (280 mg) was flash-chromatographed (25 g, 25% AcOEt in hexane) to give **25** (60 mg).

(3a*R*,7a*S*)-7a-Methyl-1-[1-(4-methyl-4-trimethylsilanyloxy-3-*oxo*-pentyl)-cyclopropyl]-3a,4,5,6,7,7a-hexahydro-3*H*-inden-4-one (26). To a stirred suspension of (100 mg, 0.33 mmol) and celite (0.4 g) in dichloromethane (5 mL) at room temperature wad added pyridinium dichromate (0.25 g, 0.66 mmol). The resulting mixture was stirred for 3 h filtered through silica gel (5 g), and then silica gel pad was washed with 20% ethyl acetate in hexane. The combined filtrate and washes were evaporated to give a crude **26** (96 mg). This material was taken up in dichloromethane (4 mL), and trimethylsilyl-imidazole (0.1 mL, 0.75 mmol) was added. The resulting mixture was stirred for 2.5 h, filtered through silica gel (10 g), and the silica gel pad was washed with 10% ethyl acetate in hexane. The combined filtrate and washes were evaporated to give **26** (100 mg, 0.27 mmol, 82%).

1α,25-Dihydroxy-16-ene-20-cyclopropyl-24-*oxo*-cholecalciferol (14). To a stirred solution of **27** (310 mg, 0.53 mmol) in tetrahydrofuran (2 mL) at −78 °C was added *n*-BuLi (0.34 mL, 0.54 mmol). The resulting mixture was stirred for 10 min and solution of **26** (95 mg, 0.25 mmol, in tetrahydrofuran (2 mL) was added dropwise. The reaction mixture was stirred at −72 °C for 3.5 h, diluted with hexane (25 mL), washed brine (20 mL), dried over Na_2SO_4, and evaporated. The residue (850 mg) was flash-chromatographed (1:9 EtOAc - hexane) to give 1α,3β-di(*tert*-butyl-dimethyl-silanyloxy)-25-trimethylsilanyloxy-16-ene-20-cyclopropyl-24-*oxo*-cholecalciferol (152 mg, 0.21 mmol). This material was dissolved in a tetrabutylammonium fluoride solution (3 mL, 1 M solution in THF), and the solution was stirred for 40 h, diluted with ethyl acetate (25 mL), washed with water (5−20 mL) and brine (20 mL), dried over Na_2SO_4, and evaporated. The residue (130 mg) was flash-chromatographed (2:1 EtOAc−hexane and ethyl acetate) to give the **14** (74 mg, 0.17 mmol, 85%); $[\alpha]^{30}_D$= −3.5 $CHCl_3$, c 0.4; UV λ_{max} (EtOH): 241 nm (ε 11080), 273 nm (ε 13283). ^{1}H NMR, 400 MHz (DMSO): 6.19 (1H, d, J = 11.3 Hz), 6.07 (1H, d, J = 11.3 Hz), 5.36 (1H, s), 5.24 (1H, s), 4.77 (1H, s), 4.19 (1H, m), 3.99 (1H, m), 2.76 (1H, m), 2.64 (2H, m), 2.39−1.24 (17H, m), 1.14 (3H, s), 1.13 (3H, s), 0.73 (3H, s),0.64−0.26 (4H, m). ^{13}C NMR (DMSO-d_6): 215.68, 156.33, 149.42, 139.29, 135.98,

124.45, 122.37, 117.73, 109.77, 75.89, 68.35, 65.15, 58.90, 49.59, 44.83, 43.11, 34.94, 33.85, 30.93, 28.80, 27.99, 26.53, 26.50, 23.12, 20.87, 17.50, 12.75, 10.00. HRMS (ES) calcd for $C_{28}H_{40}O_4$ M + Na: 463.2819; obsd M + Na: 463.2818.

Biological Studies. Compound 1 and Vitamin D Analogues. Purity of all compounds was determined by NMR spectra and was found to be ≥95%.

Crystalline 1,25$(OH)_2D_3$ (**1**) and its analogues were reconstituted in absolute ethanol, at the concentration of 1 mg/mL and stored in concentrated solutions at −80 °C under nitrogen atmosphere. **1** and its analogues were freshly diluted before each experiment, and the ethanol concentration in the test conditions did not exceed 0.00025%.

Mice. Eight-week-old C57BL/6 mice (Charles River, Italy) were housed in plastic cages with water absorbent bedding. Litter was changed at least twice a week. The animal room was temperature controlled and had a 12 h light/dark cycle. Food and water were supplied ad libitum. All procedures were reviewed and approved by local ethical committee.

Assessment of the MTD. Eight-week-old female C57BL/6 mice (3 mice/group) were dosed orally (0.1 mL/mouse) with various concentrations of VDR agonists daily for four days. Analogues were formulated in miglyol for a final concentration of 0.01, 0.03, 0.1 0.3, 1, 3, 10 30, 100, and 300 μg/kg when given at 0.1 mL/mouse po. Blood for serum calcium assay was drawn by tail bleed on day five, the final day of the study. Serum calcium levels were determined using a colorimetric assay (Sigma Diagnostics, procedure no. 597). The highest dose of analogue tolerated without inducing hypercalcemia (serum calcium >10.7 mg/dL) was taken as the MTD and expressed in μg/kg.

Cell Cultures. PBMC were separated from buffy coats by Ficoll gradient. For the bidirectional MLR, the same number (3×10^5/200 μL/well) of allogeneic PBMC from two different donors were cocultured in 96-well flat-bottom plates in RPMI 1640 with Glutamax and 5% (v/v) heat inactivated Fetal Clone-1 (FC-1, Charles River) with 1% non essential amino acids, 0.5 mg/mL gentamicin, and 1 mM of sodium pyruvate. After 5 days, proliferation and cytokine production were measured. For LPS-activated cells, PBMCs (2×10^5/200 μL/well) were cultured in RPMI 1640 with Glutamax and 10% (v/v) heat inactivated fetal bovine serum (FBS, Charles River) with 1% non essential amino acids, 0.5 mg/mL gentamicin, and 1 mM of sodium pyruvate in 96-well flat-bottom plates in presence of 100 ng/mL of LPS from *Escherichia coli* 0111:B4 (Sigma-Aldrich, USA). After 24 h, cytokine production was measured. THP-1 cells were maintain in culture in phenol red-free RPMI 1640 with Glutamax and 10% (v/v) heat inactivated FBS with 0.1 mg/mL streptomycin and 100 U/mL of penicillin. Prior to the treatment, THP-1 (10^6/mL) were grown overnight in phenol red-free RPMI 1640 with Glutamax and 5% (v/v) charcoal-treated heat inactivated FBS with 0.1 mg/mL streptomycin and 100 U/mL of penicillin. Then after 4 h treatment with the corresponding concentration of VDR agonist, mRNAs were extracted. CAOV cells were maintained in McCoy's culture media supplemented with 10% FCS. For the metabolism studies $3-10^6$ cells were seeded in T150 culture bottles and were grown to confluence.

Cytokine Quantification. ELISA for human IFN-γ, TNF-α, and IL-6 were performed using mAb pairs and standards provided in the BD OptEIA Human ELISA set (BD Pharmingen, San Diego, CA) according to the manufacturer's procedure. ELISA for human IL-12/IL-23p40 was performed using commercially available mAbs and standards (BD Pharmingen, San Diego, CA) according to the manufacturer's instructions.

Real-Time Quantitative RT-PCR. RNA was extracted using the RNeasy kit (Qiagen, Hilden, Germany) according to the manufacturer's procedure. Reverse transcription was performed, and real-time quantitative RT-PCR of total cDNA using specific primers was carried out employing an ABI PRISM 7000 sequence detection system (Applied Biosystems, USA) and TaqMan chemistry. The primers used are commercially available from Applied Biosystems as assays-on-demand.

Relative quantification of target cDNA was determined by arbitrarily setting the control value to 1 and changes in cDNA content of a sample were expressed as a multiple thereof. Differences in cDNA input were corrected by normalizing to glyceraldehyde 3-phosphate dehydrogenase (*GAPDH*) signal. To exclude amplification of genomic DNA, RNA samples were treated with DNase (Sigma-Aldrich, USA).

Metabolism Studies and HPLC. Confluent CAOV cells were incubated with 1 μM concentrations of **1** and **13** in 50 mL media containing 10% FCS. The incubations were carried out at 37 °C in a humidified atmosphere under 5% CO_2 and were stopped at 24 h with 10 mL of methanol. The lipids from both cells and media were extracted for HPLC analysis using the extraction procedure described earlier.[11] The lipid extract of media and cells was subjected directly to high performance liquid chromatography (HPLC) using the chromatographic conditions described in the legend of Figure 2. The various vitamin D_3 metabolites were monitored by a photodiode array detector, and the metabolites were identified based on the elution positions of known standards.

GC/MS Analysis. GC-MS analysis was performed using an Agilent GC System 6890 equipped with a mass selective detector MSD5973. Prior to analysis, the vitamin D_3 compounds were trimethylsilylated in a 1:1 acetonitrile:Tri-Sil TBT (Pierce, Rockford, IL) mixture and incubated at 70 °C for 15 min to ensure complete derivatization. The final concentration of each trimethylsilylated compound was 50 μg/mL. All analyses were performed on a HP-Ultra1 GC column (25 mm × 0.2 mm × 0.11 μm film thickness, 100% dimethylpolysiloxane), using UHP helium as a carrier gas at a flow rate of 0.8 mL/min. Oven temperature program was as follows: initial temperature 150 °C, then 10 °C/min until reaching a final temperature of 300 °C, which was held for 5 min. Full scan electron spectra across the mass range of m/z 50−800 were acquired in each run and the published spectra were averaged and background subtracted.

Statistics

Data were analyzed with graph prism version 5.0 and curves were generated with the appropriate nonlinear fit regression. Statistical significance was determined by a two-way analysis of variance (ANOVA), followed by Bonferroni t-test. Differences were considered significant at $P < 0.05$.

Acknowledgment. This paper is dedicated to Professor Anthony W. Norman in recognition of his many fundamental contributions to vitamin D research, including the discovery of 1α,25-dihydroxy D_3 and its first clinical use in treatment of renal osteodystrophy. This work was supported in part by the European Community grant NucSys to L.A. (MRTN-CT-019496).

References

(1) Adorini, L.; Penna, G. Control of autoimmune diseases by the vitamin D endocrine system. *Nat. Clin. Pract. Rheumatol.* **2008**, *4*, 404–412.
(2) Evans, R. M. The nuclear receptor superfamily: a rosetta stone for physiology. *Mol. Endocrinol.* **2005**, *19*, 1429–1438.
(3) Carlberg, C. Current understanding of the function of the nuclear vitamin D receptor in response to its natural and synthetic ligands. *Recent Results Cancer Res.* **2003**, *164*, 29–42.
(4) Fogh, K.; Kragballe, K. New vitamin D analogs in psoriasis. *Curr. Drug Targets Inflamm. Allergy* **2004**, *3*, 199–204.
(5) Cantorna, M. T. Vitamin D and its role in immunology: multiple sclerosis, and inflammatory bowel disease. *Prog. Biophys. Mol. Biol.* **2006**, *92*, 60–64.
(6) Campbell, M. J.; Adorini, L. The vitamin D receptor as a therapeutic target. *Expert Opin. Ther. Targets* **2006**, *10*, 735–748.
(7) Penna, G.; Amuchastegui, S.; Cossetti, C.; Aquilano, F.; Mariani, R.; Sanvito, F.; Doglioni, C.; Adorini, L. Treatment of experimental autoimmune prostatitis in nonobese diabetic mice by the vitamin D receptor agonist elocalcitol. *J. Immunol.* **2006**, *177*, 8504–8511.
(8) Bouillon, R.; Okamura, W.; Norman, A. Structure−function relationships in the vitamin D endocrine system. *Endocr. Rev.* **1995**, *16*, 200–257.

(9) Mathieu, C.; Adorini, L. The coming of age of 1,25-dihydroxyvitamin D(3) analogs as immunomodulatory agents. *Trends Mol. Med.* **2002**, *8*, 174–179.
(10) Nagpal, S.; Na, S.; Rathnachalam, R. Noncalcemic actions of vitamin D receptor ligands. *Endocr. Rev.* **2005**, *26*, 662–687.
(11) Crescioli, C.; Ferruzzi, P.; Caporali, A.; Scaltriti, M.; Bettuzzi, S.; Mancina, R.; Gelmini, S.; Serio, M.; Villari, D.; Vannelli, G. B.; Colli, E.; Adorini, L.; Maggi, M. Inhibition of prostate cell growth by **13**8, a **1** analogue selected for a phase II clinical trial in patients with benign prostate hyperplasia. *Eur. J. Endocrinol.* **2004**, *150*, 591–603.
(12) Adorini, L.; Penna, G.; Amuchastegui, S.; Cossetti, C.; Aquilano, F.; Mariani, R.; Fibbi, B.; Morelli, A.; Uskokovic, M.; Colli, E.; Maggi, M. Inhibition of prostate growth and inflammation by the vitamin D receptor agonist elocalcitol. *J. Steroid Biochem. Mol. Biol.* **2007**, *103*, 689–693.
(13) Colli, E.; Rigatti, P.; Montorsi, F.; Artibani, W.; Petta, S.; Mondaini, N.; Scarpa, R.; Usai, P.; Olivieri, L.; Maggi, M. BXL628, a novel vitamin D3 analog arrests prostate growth in patients with benign prostatic hyperplasia: a randomized clinical trial. *Eur. Urol.* **2006**, *49*, 82–86.
(14) Uskokovic, M. R.; Manchand, P.; Marczak, S.; Maehr, H.; Jankowski, P.; Adorini, L.; Reddy, G. S. C-20 cyclopropyl vitamin D3 analogs. *Curr. Top. Med. Chem.* **2006**, *6*, 1289–1296.
(15) Lemire, J. M.; Archer, D. C.; Reddy, G. S. 1,25-Dihydroxy-24-*oxo*-16-ene-vitamin D3, a renal metabolite of the vitamin D analog 1,25-dihydroxy-16-ene-vitamin D3, exerts immunosuppressive activity equal to its parent without causing hypercalcemia in vivo. *Endocrinology* **1994**, *135*, 2818–2821.
(16) Siu-Caldera, M. L.; Clark, J. W.; Santos-Moore, A.; Peleg, S.; Liu, Y. Y.; Uskokovic, M. R.; Sharma, S.; Reddy, G. S. 1α,25-dihydroxy-24-*oxo*-16-ene vitamin D3, a metabolite of a synthetic vitamin D3 analog, 1α,25-dihydroxy-16-ene vitamin D3, is equipotent to its parent in modulating growth and differentiation of human leukemic cells. *J. Steroid. Biochem. Mol. Biol.* **1996**, *59*, 405–412.
(17) Siu-Caldera, M. L.; Rao, D. S.; Astecker, N.; Weiskopf, A.; Vouros, P.; Konno, K.; Fujishima, T.; Takayama, H.; Peleg, S.; Reddy, G. S. Tissue specific metabolism of 1α,25-dihydroxy-20-epi-vitamin D3 into new metabolites with significant biological activity: studies in rat osteosarcoma cells (UMR 106 and ROS 17/2.8). *J. Cell. Biochem.* **2001**, *82*, 599–609.
(18) Tocchini-Valentini, G.; Rochel, N.; Wurtz, J. M.; Mitschler, A.; Moras, D. Crystal structures of the vitamin D receptor complexed to superagonist 20-epi ligands. *Proc. Natl. Acad. Sci. U.S.A* **2001**, *98*, 5491–5496.
(19) Clerici, M.; Stocks, N. I.; Zajac, R. A.; Boswell, R. N.; Lucey, D. R.; Via, C. S.; Shearer, G. M. Detection of three distinct patterns of T helper cell dysfunction in asymptomatic, human immunodeficiency virus-seropositive patients. Independence of CD4+ cell numbers and clinical staging. *J. Clin. Invest.* **1989**, *84*, 1892–1899.
(20) Kerman, R. H.; Susskind, B.; Katz, S. M.; Van Buren, C. T.; Kahan, B. D. Postrenal transplant MLR hypo-responders have fewer rejections and better graft survival than MLR hyper-responders. *Transplant. Proc.* **1997**, *29*, 1410–1411.
(21) Matsumoto, S.; Marui, S.; Shiho, O.; Tsukamoto, K.; Yoshimura, N.; Oka, T. A novel immunosuppressant, IR-1116, which has a different biological mechanism from that of cyclosporine A. *Eur. J. Immunol.* **1993**, *23*, 2121–2128.
(22) Cippitelli, M.; Santoni, A. Vitamin D3: a transcriptional modulator of the interferon-γ gene. *Eur. J. Immunol.* **1998**, *28*, 3017–3030.
(23) Romagnani, S. Lymphokine production by human T cells in disease states. *Annu. Rev. Immunol.* **1994**, *12*, 227–257.
(24) Lemire, J. M.; Archer, D. C.; Beck, L.; Spiegelberg, H. L. Immunosuppressive actions of 1,25-dihydroxyvitamin D3: preferential inhibition of Th1 functions. *J. Nutr.* **1995**, *125*, 1704S–1708S.
(25) Mattner, F.; Smiroldo, S.; Galbiati, F.; Muller, M.; Di Lucia, P.; Poliani, P. L.; Martino, G.; Panina-Bordignon, P.; Adorini, L. Inhibition of Th1 development and treatment of chronic-relapsing experimental allergic encephalomyelitis by a non-hypercalcemic analogue of 1,25-dihydroxyvitamin D(3). *Eur. J. Immunol.* **2000**, *30*, 498–508.
(26) Akira, S.; Takeda, K. Toll-like receptor signalling. *Nat. Rev. Immunol.* **2004**, *4*, 499–511.
(27) Medzhitov, R. Recognition of microorganisms and activation of the immune response. *Nature* **2007**, *449*, 819–826.
(28) Bradley, J. R. TNF-mediated inflammatory disease. *J. Pathol.* **2008**, *214*, 149–160.
(29) Feldmann, M.; Steinman, L. Design of effective immunotherapy for human autoimmunity. *Nature* **2005**, *435*, 612–619.
(30) Gately, M. K.; Renzetti, L. M.; Magram, J.; Stern, A. S.; Adorini, L.; Gubler, U.; Presky, D. H. The interleukin-12/interleukin-12-receptor system: role in normal and pathologic immune responses. *Annu. Rev. Immunol.* **1998**, *16*, 495–512.
(31) Langrish, C. L.; McKenzie, B. S.; Wilson, N. J.; de Waal Malefyt, R.; Kastelein, R. A.; Cua, D. J. IL-12 and IL-23: master regulators of innate and adaptive immunity. *Immunol. Rev.* **2004**, *202*, 96–105.
(32) Bettelli, E.; Korn, T.; Oukka, M.; Kuchroo, V. K. Induction and effector functions of T(H)17 cells. *Nature* **2008**, *453*, 1051–1057.
(33) Horst, R. L.; Reinhardt, T. A.; Reddy, G. S. Vitamin D metabolism. In *Vitamin D*; Feldman, D., Glorieux, F. H., Pike, J. W., Eds.; Academic Press, Inc.: New York, 2005; pp 15−35.
(34) Omdahl, J. L.; May, B. The 25-Hydroxyvitamin D 24-Hydroxylase. In *Vitamin D*; Feldman, D., Glorieux, F. H., Pike, J. W., Eds.; Academic Press: New York, 2005; pp 85−104.
(35) Wang, T. T.; Nestel, F. P.; Bourdeau, V.; Nagai, Y.; Wang, Q.; Liao, J.; Tavera-Mendoza, L.; Lin, R.; Hanrahan, J. W.; Mader, S.; White, J. H. Cutting edge: 1,25-dihydroxyvitamin D3 is a direct inducer of antimicrobial peptide gene expression. *J. Immunol.* **2004**, *173*, 2909–2912.
(36) Liu, P. T.; Stenger, S.; Li, H.; Wenzel, L.; Tan, B. H.; Krutzik, S. R.; Ochoa, M. T.; Schauber, J.; Wu, K.; Meinken, C.; Kamen, D. L.; Wagner, M.; Bals, R.; Steinmeyer, A.; Zugel, U.; Gallo, R. L.; Eisenberg, D.; Hewison, M.; Hollis, B. W.; Adams, J. S.; Bloom, B. R.; Modlin, R. L. Toll-like receptor triggering of a vitamin D-mediated human antimicrobial response. *Science* **2006**, *311*, 1770–1773.
(37) Schauber, J.; Dorschner, R. A.; Coda, A. B.; Buchau, A. S.; Liu, P. T.; Kiken, D.; Helfrich, Y. R.; Kang, S.; Elalieh, H. Z.; Steinmeyer, A.; Zugel, U.; Bikle, D. D.; Modlin, R. L.; Gallo, R. L. Injury enhances TLR2 function and antimicrobial peptide expression through a vitamin D-dependent mechanism. *J. Clin. Invest.* **2007**, *117*, 803–811.
(38) Uskokovic, M. R.; Marczak, S.; Jankowski, P.; Adorini, L. Deuteroalkyl vitamin D3 compounds and their pharmaceutical compositions. WO200738250, 2007.

JM801365A